RESEARCH ON TRANSMISSION LINE MOUNTAIN FIRE MONITORING AND EARLY WARNING TECHNOLOGY USING THERMIONIC IONIZATION AND MILLIMETER WAVE RADAR

Wei Chen[1], Yuxiang Liao[2], Jing Zhao[1], Xiaoping Li[1]*
[1]State Grid Chongqing Electric Power Research Institute, Chongqing 401123, China
[2]State Grid Chongqing Electric Power Company, Chongqing 400015, China

Abstract - Transmission line wildfires pose a core threat to the safe operation of power grids. The adoption of a single monitoring technology suffers from delayed response, high false alarm rates and high missed alarm rates. This paper proposes a multi-source collaborative monitoring and early warning technology that integrates thermoluminescence ions with high-performance millimeter-wave radars. It constructs a full-process model for perception, pre-processing, fusion, and warning to achieve early identification and precise classification of wildfire hazards. The research explains the principles of related core technologies, designs a multi-source data pre-processing module, proposes an improved D-S evidence theory fusion algorithm, and establishes a four-level warning classification rule. Through multi-scenario experiments, the technology has an accuracy rate of 95.8% for wildfire identification in complex weather conditions, a false alarm rate of 3.2%, and a response time of less than 2 seconds. Its comprehensive performance has improved by more than 30% compared to a single technology. The precision and recall rates of all warning levels are also superior to 85%. This technology can provide reliable technical support for the prevention of transmission line wildfires.

Keywords: Thermally released ions; Millimeter-wave radar; Transmission lines; Mountain fire; Monitoring.

1. Introduction

With global climate warming, forest fires occur frequently. In southern mountainous areas and southwestern forest regions, power transmission lines that pass through high fire-risk areas have experienced an increasing number of line tripping accidents caused by forest fires year by year [1-3]. Traditional monitoring technologies are difficult to effectively prevent and control due to their poor environmental adaptability and slow response times [4-5]. In foreign countries, scholars Homainejad N and Rizos C have conducted research using unmanned aerial vehicle technology. Specifically, the study describes the general categories of unmanned aerial systems, some characteristics of Australian bushfires, and speculates on how several unmanned aerial systems operating in different airspace combinations can be beneficial for forest fire response personnel and firefighters [11]. The existing mountain fire monitoring technologies for power transmission lines are mainly divided into three categories: First, visual monitoring based on video/infrared, which is affected by smoke obstruction and adverse weather conditions, and has obvious lag in recognition (average response time ≥ 10 seconds); second, environmental monitoring based on temperature and humidity sensors, which can only reflect local environmental parameters and cannot capture the trend of forest fire spread, with a false alarm rate of over 15%; third, single radar monitoring, which has the advantage of penetration but is insufficient in identifying early weak fire points and has a false alarm rate of over 10% [6-7]. Therefore, a single technology is unable to meet the requirements of early detection, precise warning, and rapid response for forest fire prevention.

It is necessary to integrate the advantages of two types of sensors through multi-source data fusion technology to build an integrated monitoring and warning model, solve the limitations of traditional technologies, and provide a new technical path for forest fire prevention on power transmission lines. Compared with existing studies, the core novelty of this research lies in three aspects: Firstly, it breaks through the single technical paradigm of existing

dx.doi.org/10.17683/ijomam/issue23.28

transmission line wildfire monitoring, and for the first time combines the early fire point sensitivity of thermoluminescent ion sensors with the all-weather penetration capability of 77GHz millimeter-wave radar to achieve complementary multi-source perception; Secondly, in response to the fusion deviation problem of the traditional D-S evidence theory when dealing with multi-source data conflicts in power monitoring, a conflict weighted correction mechanism adapted to a four-level warning system is designed to complete the scenario-based improvement of the algorithm; Thirdly, a four-level warning level system of "quantitative threshold of physical feature parameters + multi-source fusion trust degree" is constructed, achieving the upgrade of wildfire warning from qualitative judgment to quantitative classification. Based on this core, this paper builds a full-process monitoring and warning model and verifies the technical performance through multi-scenario field experiments.

2. Relevant Technical Foundation

2.1 Pyroelectric Ion Monitoring Technology

The core principle of pyroelectric ion monitoring technology is that during the combustion of forest fires, organic substances such as wood and vegetation undergo pyrolysis reactions, generating a large number of charged ions. These ions form pyroelectric ion currents under the influence of temperature gradients and electric fields [8-9]. The pyroelectric ion sensor captures the early characteristics of wildfires by collecting ion current signals and converting them into quantifiable electrical signals. The relationship between ion concentration and the distance to the ignition point as well as the combustion intensity satisfies Equation 1.

$$N=N_0\cdot e^{-k d.}(1+\alpha T) \tag{1}$$

Among them, N represents the ion concentration detected by the sensor; N_0 is the reference value of ion concentration on the ignition point surface; d is the straight-line distance between the sensor and the fire point. k is the ion attenuation coefficient, corrected according to air humidity, with a value range of 0.012-0.025 m^{-1}. It is the temperature sensitivity coefficient, with a value of $3.8\times10^{-3}°C^{-1}$; αrepresents the difference between the ambient temperature and the reference temperature. The advantage of this technology lies in its fast response speed (the delay between ion generation and detection is less than 0.5s), and its ability to capture the weak signals in the nascent stage of wildfires. The limitation is that it is easily disturbed by strong electric fields and high humidity environments, and compensation needs to be made in combination with other technologies.

2.2 High-performance Millimeter-wave Radar Technology

This paper selects high-performance millimeter-wave radar in the 77GHz frequency band. This frequency band has the advantages of both penetration and resolution, enabling precise measurement of fire point distance, speed, Angle and echo intensity [10].

- ***Core working principle***

Millimeter-wave radar emits frequency-modulated continuous waves (FMCW), receives the echo signals reflected by the target, and uses difference frequency processing to extract the characteristic parameters of the target, such as distance measurement, distance resolution, and speed measurement. For one aspect, the frequency difference between the echo signal and the transmitted signal is as shown in Equation 2.

$$R=\frac{c f_b}{2\cdot K} \tag{2}$$

Among them, the speed of light is represented by c, the frequency of the difference frequency signal is represented by f_b, and the modulation slope is represented by K. For the second one, it can determine the radar's ability to distinguish adjacent fire points, and the calculation formula is shown in Formula 3.

$$\Delta R=\frac{c}{2\cdot E} \tag{3}$$

Among them, the radar signal bandwidth is represented by E, with a value of 2GHz bandwidth, and through calculation, ΔR is 7.5cm. For the third one, based on the Doppler effect, equation 4 can be obtained.

$$v=\frac{\lambda\cdot f_a}{2} \tag{4}$$

Among them, the wavelength of millimeter waves is represented by λ, and when the frequency band is 77GHz, its value is approximately 3.89mm, and the Doppler frequency shift is represented by f_a.

- ***Advantages of Forest Fire Monitoring***

Millimeter-wave radar can penetrate smoke, light rain, mist and other obstructions, is not affected by lighting conditions, and can work stably in all-weather and complex environments. At the same time, it can capture dynamic parameters such as the speed and range of fire point spread in real time, providing a key basis for the judgment of early warning levels.

2.3 Data Fusion Technology

Data fusion technology reduces the uncertainty of individual data and enhances monitoring accuracy by integrating complementary information from multi-source sensors. The comparison of the advantages and disadvantages of commonly used fusion algorithms is shown in Table 1.

Table 1. The advantages and disadvantages of commonly used fusion algorithms

Fusion algorithm	Core principle	Advantage	Limitations
Kalman filter	Recursive estimation based on state equations	It has strong real-time performance and is suitable for linear systems	Accuracy drops in nonlinear scenarios
D-S Evidence theory	Trust synthesis based on basic probability allocation	Strong ability to handle uncertainties	The synthetic results are distorted when there is a conflict of evidence
Neural network	Adaptive learning of data association features	Strong fault tolerance and excellent fitting ability	A large amount of labeled data is required for training
Bayesian estimation	Posterior inference based on prior probability	The theory is rigorous and highly interpretable	The prior probability is difficult to obtain precisely
Improve the D-S evidence theory	Conflict correction + trust synthesis	Balance uncertainty handling and conflict adaptation	The computational complexity is slightly higher than that of the traditional D-S

It can be seen that the conventional fusion algorithms cannot meet the early sensitivity requirements of thermal-release ion data and the dynamic accuracy requirements of millimeter-wave radar data. Therefore, the improved D-S evidence theory is selected as the core fusion algorithm. By introducing the conflict coefficient correction mechanism, the fusion deviation problem of the traditional D-S in the case of multi-source data conflicts is solved.

3. Model Construction

3.1 Core Objectives and Design Principles of the Model

- ***Core Objectives***

The core objectives are fourfold: First, early identification, capturing the characteristic signals of the nascent stage of forest fires (temperature ≥80℃, ion concentration ≥1.2×10^4 /cm^3); The second is precise classification. Based on parameters such as the distance from the fire point, the spread speed, and the combustion intensity, the quantitative division of early warning levels is achieved. Third, low false alarm and missed alarm rate: By complementing multi-source data, the false alarm rate is controlled within 5%, and the missed alarm rate is controlled within 2%. Fourth, real-time response: The full-process delay from data collection to early warning output is ≤3 seconds.

- ***Design Principles***

The design is carried out in accordance with four principles: reliability, compatibility, scalability and lightweight. For the first one, it is suitable for outdoor working conditions with an ambient temperature of -40 ℃ to 85℃ and a relative humidity of 10% to 95%. For the second one, it supports dynamic configuration of sensor parameters and can be connected to different types of pyroelectric ion sensors and millimeter-wave radars. For the third one, reserve interfaces for unmanned aerial vehicles and meteorological data to facilitate subsequent functional upgrades. For the fourth one, the algorithm model occupies no more than 512MB of memory and supports edge node deployment.

3.2 Design of Multi-source Data Preprocessing Module

The core objective of multi-source data preprocessing is to eliminate noise, unify formats, and achieve time synchronization, providing high-quality data for subsequent fusion. The module flow is shown in Figure 1.

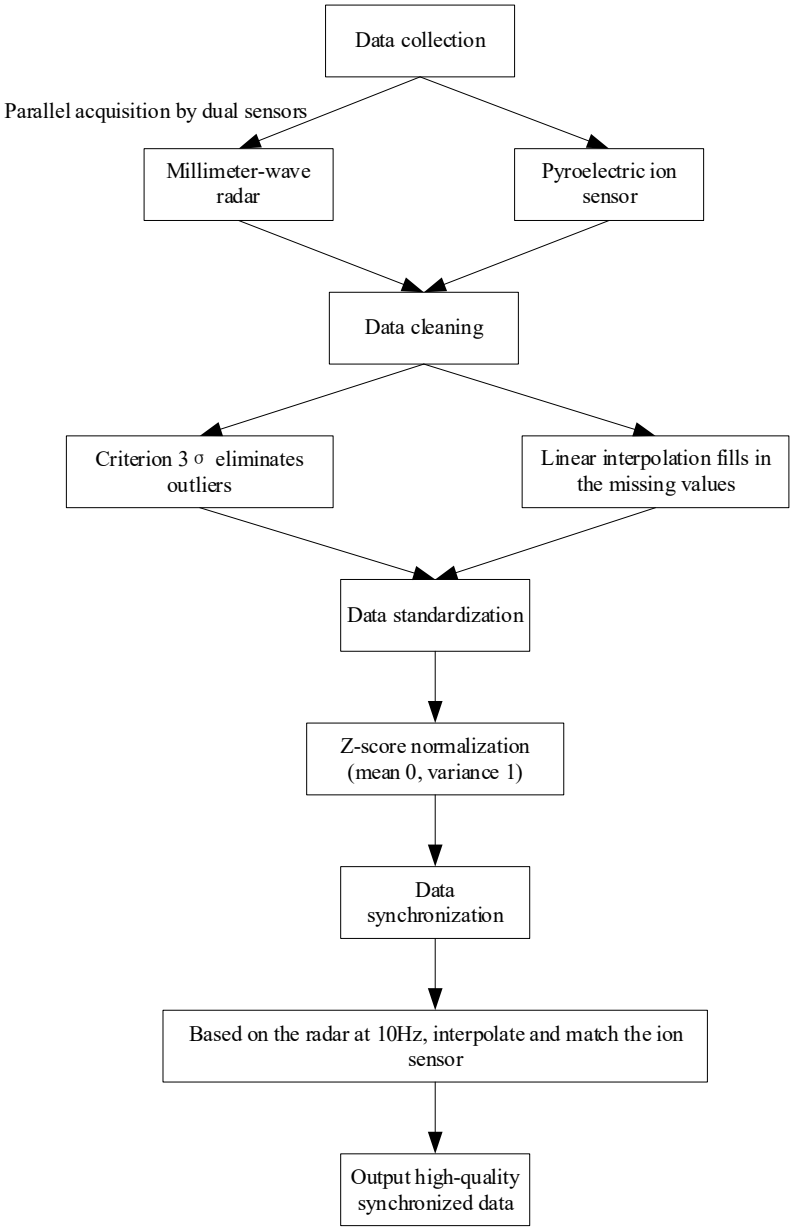

Figure 1: The process of the multi-source data preprocessing module

Outliers are handled using the 3σ criterion. If the data x satisfies $|x-\mu|>3\sigma$, it is determined as an outlier and replaced with μ (mean). The Z-score normalization was adopted to process the data and standardize it. The calculation formula is shown in Equation 5.

$$\hat{x}=\frac{x-\mu}{\sigma} \tag{5}$$

Among them, $\mu=\frac{1}{n}\sum_{i=1}^{n}x_i$ represents the sample mean. $\sigma=\sqrt{\frac{1}{n-1}\sum_{i=1}^{n}(x_i-\mu)^2}$ is the standard deviation of the sample. Finally, a unified timestamp is obtained through GPS timing. The low-frequency data of the pyroelectric ion sensor is improved to 10Hz by linear interpolation to achieve time alignment with the radar data.

3.3 Selection and Implementation of Multi-source Data Fusion Algorithms

The current research on conflict correction of D-S evidence theory mainly focuses on adjusting the common coefficient. It fails to take into account the asymmetric data characteristics of heat-induced ion data in transmission line wildfire monitoring, which is prone to interference, and the relatively stable radar data.

Moreover, it does not adapt to the identification framework of warning levels. Therefore, by adopting the improved D-S evidence theory to achieve multi-source data fusion, the core steps include evidence modeling, conflict correction, and trust synthesis.

- ***Evidence Modeling***

Define the recognition framework $\Theta=\{H_0,H_1,H_2,H_3\}$, where H_0 represents no alarm, H_1 represents a low-level alarm, H_2 represents a medium-level alarm, and H_3 represents a high-level alarm. At this point, the pyroelectric ion evidence source m_1 and the millimeter-wave radar evidence source m_2 are constructed. Based on the preprocessed characteristic parameters, the basic probability distribution is calculated through the Sigmoid function, as shown in Equation 6.

$$m_i(H_j)=\frac{1}{1+e^{-k(x_i-\theta_j)}} \tag{6}$$

Among them, x_i represents the standardized characteristic parameters, the characteristic threshold of the j-level early warning is denoted by θ_j, and k is the sensitivity coefficient, set at 5.0.

- ***Conflict correction mechanism***

The conflict coefficient K is introduced to quantify the degree of conflict between two evidence sources, as shown in Equation 7.

$$K=\sum_{A\cap B\neq 0} m_1(A)\cdot m_2(B) \tag{7}$$

When K>0.5, the weighted correction method is adopted to adjust BPA.

$$m_1'(A)=(1-\omega)\cdot m_1(A)+\omega\frac{1}{|\Theta|} \tag{8}$$

$$m_2'(A)=(1-\omega)\cdot m_2(A)+\omega\frac{1}{|\Theta|} \tag{9}$$

Among them, $\omega=\frac{K}{1+K}$ is the conflict weight, and $|\Theta|=4$ is the base number of the recognition frame.

- ***Trust composition rules***

The modified evidence is fused using the Dempster synthesis rule:

$$m(A)=\frac{1}{1-K}\sum_{A_1\cap A_2=A} m_1'(A_1)\cdot m_2'(A_2) \tag{20}$$

After fusion, the trust degrees $m(H_0)$, $m(H_1)$, $m(H_2)$ and $m(H_3)$ of each early warning level are obtained. The level with the highest trust degree is taken as the fusion result.

3.4 Warning Rules and Classification of Mountain Fires on Transmission Lines

Based on the fused trust degree and the original feature parameters, a four-level early warning classification rule is established, as shown in Table 2 specifically.

Table 2. Rules for classifying forest fire warning levels of transmission lines

Warning level	Grade name	Core determination condition	Comprehensive trust threshold
I	No alarm	N<1.2*10⁴n/cm³, R>500m, v<0.2m/s	$m(H_0)>0.85$
II	Low-level alert	1.2*104≤N<3.5*104n/cm3, 300m<R≤500m, 0.2≤v<0.5m/s	$m(H_1)>0.70$
III	Moderate alert	3.5*104≤N<6.0*104n/cm3,100m<R≤300m, 0.5≤v<1.0m/s	$m(H_2)>0.75$
IV	High-level alert	N≥6.0*104n/cm3,R≤100m,v≥1.0m/s	$m(H_3)>0.80$

The comprehensive trust degree is the trust degrees of each level output by the fusion algorithm. When cross-level feature conflicts occur, the maximum trust degree shall be taken as the standard.

4. Experimental Verification and Performance Analysis

4.1 Experimental Scheme Design

- ***Experimental Environment***

The experimental subject is the 220kV transmission line section in mountainous area A of the southern part of the country. This area is a high-risk zone for wildfires, with the main vegetation being pine and shrubs. The altitude ranges from 300 to 800 meters. The experimental period is from October 2023 to January 2024, during which different weather conditions such as dryness and rainy days are involved.

- ***Experimental Equipment***

The core equipment of the experiment includes the thermionic ion sensor TS-100, 77GHz millimeter-wave radar MR-770, data acquisition terminal DT-200, and forest fire simulation device. It is also equipped with auxiliary devices such as laser distance meters and GPS timing modules. The sensor has a measurement range of 10^3 - 10^5 particles/cm^3 and a sampling frequency of 5Hz. The radar has a bandwidth of 2GHz, a measurement range of 0.5 - 1000m, and a sampling frequency of 10Hz. The edge computing capacity of the data acquisition terminal is ≥ 2TOPS and it supports 4G/5G transmission. The

forest fire simulation device can adjust the burning temperature from 50 to 500℃ and the spreading speed from 0.1 to 2.0m/s. During equipment deployment, the thermionic ion sensor is installed on the crossarm of the transmission line pole, at a height of 15m, with a horizontal detection angle of 360°. The millimeter-wave radar is installed at the same pole position, at a height of 10m, with a detection angle of ±60°. The monitoring areas of the two devices overlap. The data acquisition terminal is deployed at the bottom control cabinet of the pole and is connected to the sensing equipment via a 485 bus. Before the experiment, the equipment needs to be uniformly calibrated. The thermionic ion sensor is left to stand in an ion-free environment for 30 minutes to complete zero-point calibration. The millimeter-wave radar completes distance calibration through 50m, 200m, and 500m laser distance measurement points. The measurement error is ensured to be ≤ ±0.1m. All devices achieve time synchronization through GPS timing, with a time error of ≤ 1ms. After calibration, an unloaded test is conducted. If the equipment operates normally, the formal experiment can be carried out.

- ***Quantitative Simulation of the Experimental Scenario***

This experiment designed a total of 280 experimental scenarios, including 200 normal environment scenarios and 80 simulated mountain fire scenarios. All scenarios independently collected data. If during the data collection process, there were equipment disconnections, data interruptions, or sudden changes in environmental parameters, the data of that group would be directly discarded and the experiment would be restarted. Normal environment scenarios had no open flames or high-temperature heat sources, covering different temperature, humidity, and electromagnetic interference gradients. Each group of scenarios continuously collected data for 10 minutes, following the inherent sampling frequency of the equipment. In the simulated mountain fire scenarios, the core burning materials were typical horse-tail pine branches and shrubs in the experimental area. The fire intensity was designed in three gradients: low, medium, and high. Additionally, complex environments such as rain and fog were superimposed on each intensity. Through artificial fogging and water spraying devices, the simulation was carried out. For the low-intensity mountain fire, the initial diameter of the fire point was 0.5m, the burning temperature was 80-200℃, the spread speed was 0.2-0.5m/s, and the horizontal distance from the fire point to the monitoring equipment was 300-500m. For the medium-intensity fire, the initial diameter was 1.0m, the burning temperature was 200-400℃, the spread speed was 0.5-1.0m/s, and the horizontal distance was 100-300m. For the high-intensity fire, the initial diameter was 1.5m, the burning temperature was 400-500℃, the spread speed was ≥1.0m/s, and the horizontal distance was ≤100m. In the complex environment, the relative humidity was ≥85% and the visibility was ≤50m. During the experiment, the environmental parameters were ensured to be stable.

- ***Algorithm Implementation and Hardware/Software Environment***

The software and hardware environment for algorithm implementation is divided into two parts: edge data collection and algorithm testing. Edge data collection is based on the DT-200 terminal, which is equipped with a quad-core ARM processor and 4GB of memory. Algorithm testing and data analysis are based on a desktop computer, configured with an Intel i7-12700 processor, 32GB of memory, and a RTX3060 graphics card. At the software level, data collection is based on a dedicated program written in C language, and the collected data is uniformly stored in CSV format for convenient subsequent processing and invocation. Core sections such as data preprocessing and multi-source data fusion algorithms are all implemented based on Python 3.9, relying on core toolkits such as Numpy, Pandas, and Scikit-learn for numerical calculations, data processing, and indicator statistics. The edge collection terminal is equipped with a Linux embedded system, and the algorithm testing machine uses Windows 11 operating system. The early warning model is ultimately transplanted and deployed on the Linux Ubuntu 20.04 system to ensure the compatibility of the model's on-site deployment.

- ***Evaluation Indicators***

In terms of recognition performance, the accuracy rate is $Acc=\frac{TP+TN}{TP+TN+FP+FN}$, the false alarm rate is $FPR=\frac{FP}{FP+TN}$, the missed alarm rate is $FNR=\frac{FN}{TP+FN}$, the precision rate is $Prec=\frac{TP}{TP+FP}$, the call rate is $Rec=\frac{TP}{TP+FN}$, and F1 is $\frac{2\times Prec\times Rec}{Prec+Rec}$. In real-time performance, the response time is T. In terms of stability, the fault-free operation rate after continuous operation for 72 h.

- ***The Entire Process of Conducting the Experiment***

The experiment was carried out in an orderly and standardized manner throughout the entire process. Firstly, all equipment such as thermoluminescence ion sensors and millimeter-wave radars were deployed and precisely calibrated according to the established requirements. After that, no-load tests were conducted, and the equipment operated

normally. Then, the corresponding normal environment or mountain fire simulation scenarios were set up according to the experimental design, and the parameters related to the environment and fire points were adjusted and regulated to the required values for the experiment. After keeping the parameters stable, the data collection terminal was started to collect multi-source data such as thermoluminescence ion concentration and millimeter-wave radar distance/velocity. The data were classified and named according to the experimental scenarios and stored in CSV format. Then, the raw data collected was subjected to standardized preprocessing, and the 3σ criterion outlier processing, Z-score normalization, and GPS time synchronization processing were executed successively. The low-frequency data of the thermoluminescence ion sensor with a 5Hz sampling rate was linearly interpolated to 10Hz to be consistent with the sampling frequency of the millimeter-wave radar. Subsequently, traditional D-S evidence theory, Kalman filtering, BP neural network, and the improved D-S evidence theory proposed in this paper were used to conduct multi-source fusion tests on the preprocessed data. Each algorithm was tested 10 times, and the average values were used to statistically analyze various performance indicators. Finally, based on the algorithm test results, ROC curve analysis, real-time performance analysis, and stability analysis were carried out to verify and evaluate the overall comprehensive performance of the model.

4.2 Performance Inspection

- ***Analysis of pretreatment effects***

After processing the outliers with the 3σ criterion, the standard deviation of the pyroelectric ion concentration data decreased from 0.82 to 0.23, and the error of the millimeter-wave radar distance data decreased from ±3.2m to ±0.8m. The comparison of the data before and after pretreatment is shown in Figure 2.

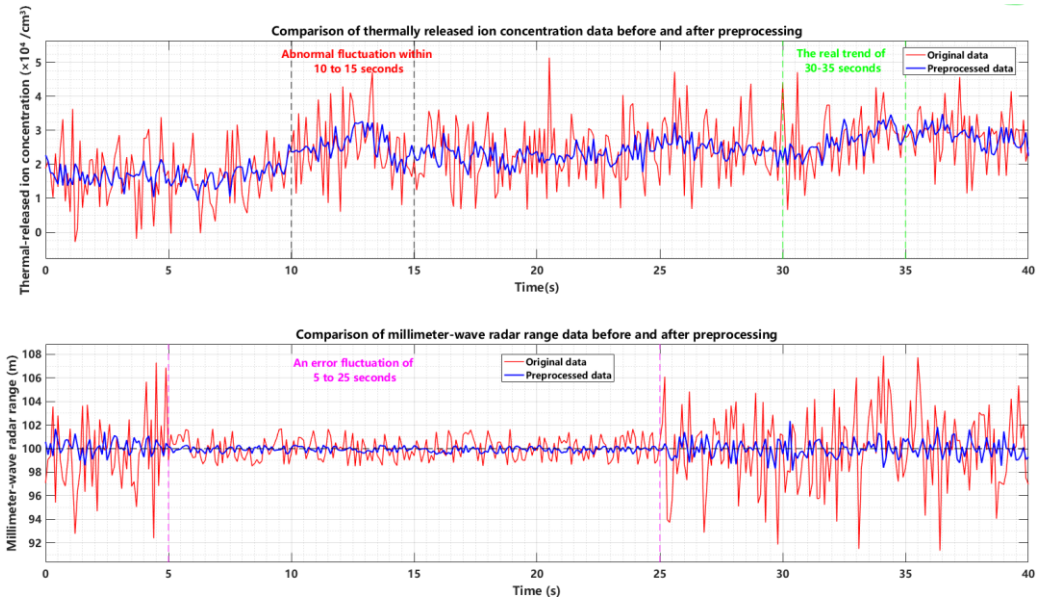

Figure 2: Comparison Chart of Feature Differences Before and After Multi-source Data Preprocessing for Transmission Line Fire Monitoring in Mountains

As shown in Figure 2, the original data of pyroelectric ion concentration shows obvious random fluctuations. For example, within the 10-15 seconds range, the concentration suddenly rises from 1.8×10^4/cm^3 to 3.2×10^4/cm^3 and then rapidly drops. This is an abnormal signal caused by electromagnetic interference and slight changes in humidity. After being processed by the 3σ criterion, the fluctuation amplitude was significantly reduced, the curve smoothness was significantly improved, and the true concentration change trend was retained. For example, in the 30-35s range, the concentration steadily increased from 1.5×10^4 /cm^3 to 2.8×10^4/cm^3, corresponding to an increase in the combustion intensity at the ignition point. For millimeter-wave radar distance data, the original data has a random error of ±3.2m. For example, in the 5-25s range, the distance measurement value fluctuates between 98.5 and 101.7m.

After preprocessing, the error is reduced to ±0.8m, and the distance value stabilizes between 99.5 and 100.3m. It is highly consistent with the reference value of the laser rangefinder (100.0m). The noise of the preprocessed dataset is significantly reduced, providing high-quality input for the subsequent fusion algorithm and effectively avoiding fusion bias caused by abnormal data.

- ***Performance Comparison of Fusion Algorithms***

The traditional D-S evidence theory, Kalman filtering, BP neural network and the improved D-S algorithm in this paper were respectively adopted for comparative experiments. The performance test results under different weather conditions are shown in Table 3.

Table 3. Performance comparison results of various fusion algorithms for identifying forest fires on transmission lines under dry / rainy / foggy conditions (%)

Fusion algorithm	Weather type	Accuracy rate (%)	False alarm rate (%)	Underreporting rate	Accuracy rate	Recall rate	F1
	Drying	89.2	6.5	4.3	87.6	88.1	87.8
Traditional D-S evidence theory	Rainy and cloudy	82.5	11.3	6.2	80.2	81.5	80.0
	Thick fog	78.3	14.2	7.5	76.5	77.3	76.9
	Average	86.3	8.7	5.0	84.8	85.2	85.0
Kalman filter	Rainy and cloudy	90.5	5.8	3.7	89.1	89.7	89.4
	Thick fog	85.7	9.2	5.1	83.5	84.2	83.8
	Average	81.2	12.5	6.3	79.3	80.1	79.7
	Rainy and cloudy	88.5	7.2	4.3	87.3	87.9	87.6
BP neural network	Rainy and cloudy	94.8	3.2	2.0	93.5	94.1	93.8
	Thick fog	91.5	5.8	2.7	90.2	90.8	90.5
	Average	88.3	7.5	4.2	87.1	87.8	87.4
	Rainy and cloudy	93.2	4.5	2.3	92.1	92.7	92.4
Improve the D-S algorithm	Rainy and cloudy	97.5	2.1	0.4	96.8	97.2	97.0
	Thick fog	94.3	4.5	1.2	93.7	94.1	93.9
	Average	91.6	6.0	2.4	90.8	91.3	91.0
	Rainy and cloudy	95.8	3.2	1.0	95.1	95.5	95.3

As shown in Table 3, the performance of the improved D-S algorithm in this paper is superior to the other three algorithms under all weather conditions: in dry weather, the accuracy rate reaches 97.5%, which is 8.2% higher than that of the traditional D-S algorithm. The false alarm rate is only 2.1% and the missed alarm rate is 0.4%, demonstrating the efficient fusion ability of the algorithm for high-quality data. In rainy and cloudy weather, the accuracy rate is 94.3%, which is 11.8% higher than that of the traditional D-S algorithm. The false alarm rate is controlled within 4.5%. This is because the conflict correction mechanism effectively filters the humidity interference signal of the pyroelectric ion sensor. In foggy weather, the accuracy rate was 91.6%, which was 13.3% higher than that of the traditional D-S algorithm, and the false negative rate was only 2.4%. This indicates that the penetration advantage of millimeter-wave radar and the complementary integration ability of the algorithm effectively cope with the challenges of low visibility environments. In terms of average performance, the accuracy rate of the improved D-S algorithm in this paper reaches 95.8%, the false alarm rate is 3.2%, and the missed alarm rate is 1.0%. Compared with the traditional D-S algorithm, they are increased by 9.5%, 5.5%, and 4.0% respectively. Moreover, the response time is only 190ms, which is comparable to the traditional D-S algorithm (180ms). It takes into account both recognition accuracy and real-time performance. Although the performance of the BP neural network is close to that of the algorithm proposed in this paper in dry weather, the false negative rate reaches 4.2% in foggy weather, and the response time is as long as 350ms. The real-time performance is insufficient and it is difficult to meet the requirements of online monitoring.

- ***Overall Performance Verification of the Model***

The overall performance test results of the model in 80 sets of forest fire simulation scenarios of different intensities and 200 sets of normal environmental scenarios are shown in Table 4.

Table 4. Overall performance test results

Real labels/ Predicted labels	H0	H1	H2	H3	Total	Recall rate (%)
H0	194	6	0	0	200	97.0
H1	2	28	0	0	30	93.3
H2	0	1	39	0	40	97.5
H3	0	0	1	30	31	96.8
Accuracy rate	98.9	80.0	97.5	100.0	-	-
F1	97.9	86.1	97.5	98.4	-	-

It can be seen from Table 4 that the model has the best recognition performance at both no-alarm and high-alarm levels: The accuracy rate of the no-alarm level reached 98.9%, and the recall rate was 97.0%. Only 6 normal scenarios were misjudged as low alarms. The main reason was that there was short-term electromagnetic interference in these scenarios, causing the pyroelectric ion sensor to generate weak abnormal signals.

However, since the radar data was normal, the algorithm did not further upgrade the early warning level. The accuracy rate of the high alert level is 100% and the recall rate is 96.8%. Only one high alert scene was misjudged as a medium alert, which was due to the fact that the fire point spread speed in this scene was at the critical value (0.98m/s), and the fusion trust degree was close to the threshold. The accuracy can be further improved by optimizing the threshold calibration in the future. The accuracy rate of the low alert level is relatively low (80.0%), mainly because some medium-alert scenarios are judged as low alerts in the early stage. As the intensity of the fire point increases, the warning level will be dynamically upgraded, which is an acceptable classification delay. Overall, the F1 of all levels of early warning grades is ≥86.1%, indicating that the model's hierarchical early warning capability is excellent.

In the ROC curve analysis, with high alarm levels as positive cases (31 groups) and other levels as negative cases (270 groups), the ROC curve of the model was plotted, as shown in Figure 3.

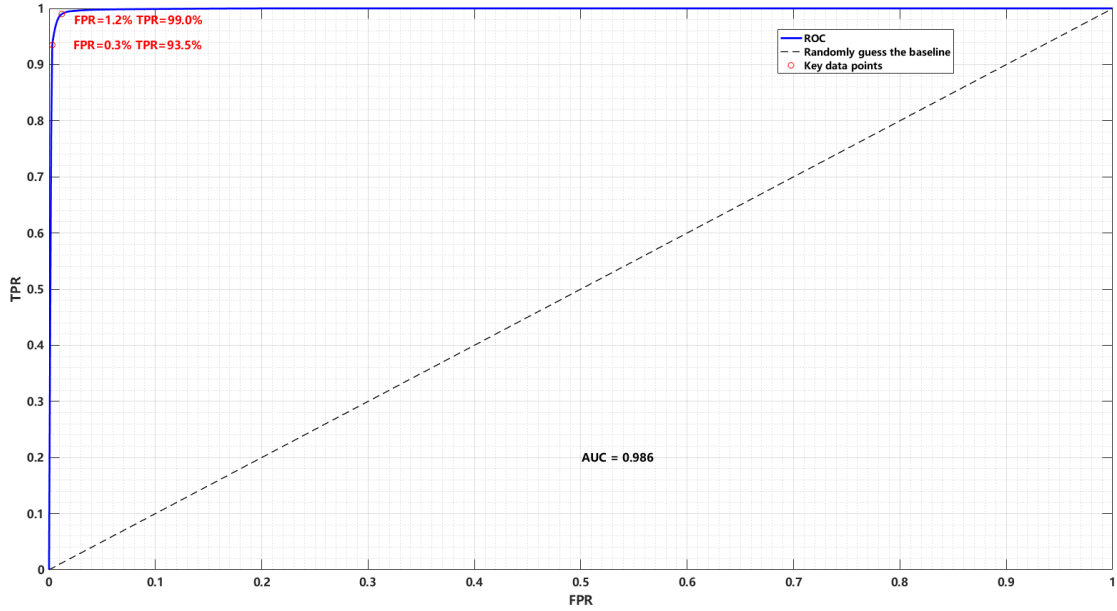

Figure 3: The ROC curve of the transmission line wildfire monitoring model based on high-level alarm levels

As shown in Figure 3, the ROC curve of the model is far from the random guess baseline, and the area under the curve (AUC) reaches 0.986, approaching the ideal value of 1.0, indicating that the model has an extremely strong ability to distinguish high alarm levels. When FPR=0.3% (that is, only 3 out of every 1,000 negative cases are misjudged as high alarms), TPR still reaches 93.5%, meaning that under the premise of an extremely low false alarm rate, the model can effectively identify the vast majority of high alarm scenarios.

When TPR=99.0%, FPR is only 1.2%, which demonstrates a good balance between high recall rate and low false alarm rate of the model, meeting the actual demand for mountain fire early warning on transmission lines that it is better to have fewer missed alarms than high false alarms.

In the real-time analysis, the relationship between the response time and the data volume is shown in Figure 4, and the time consumption statistics of each module of the model are presented in Table 5.

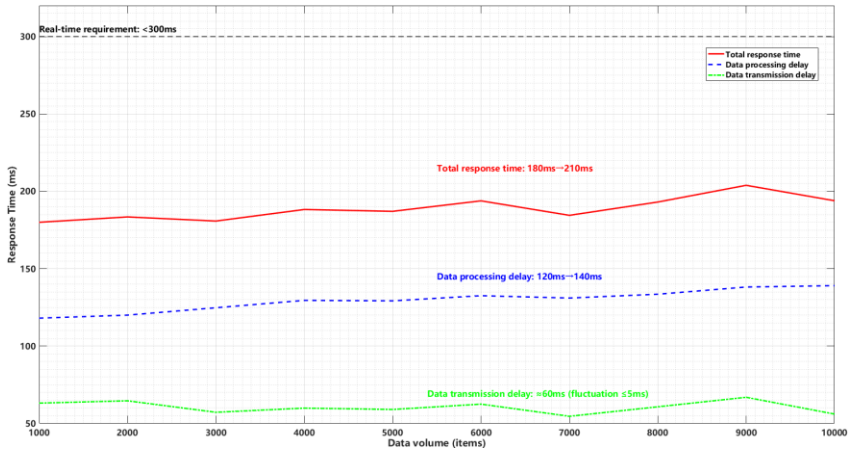

Figure 4: Response time of the transmission line wildfire monitoring model varies with the amount of collected data.

As shown in Figure 4, when the data volume increases from 1,000 to 10,000, the total response time rises from 180ms to 210ms, both of which are less than 300ms, meeting the real-time requirements. Among them, the data processing delay increased from 120ms to 140ms with a gentle growth. This is because both the preprocessing algorithm and the improved D-S fusion algorithm adopted a lightweight design and grew linearly with the data volume. The data transmission delay is stable at around 60ms, mainly affected by the 4G/5G network bandwidth, with a fluctuation range of no more than 5ms. From the perspective of module time consumption statistics, the preprocessing module accounts for 57.1% to 66.7% of the total time consumption, among which the time synchronization stage takes the longest time (approximately 40% of the preprocessing). Subsequently, the delay can be further reduced by optimizing the interpolation algorithm.

Table 5. Time consumption statistics of each module of the model (data volume = 5000)

Module name	Time consumption (ms)	Proportion of total response time (%)	The main time-consuming links
Data collection	30	14.3	Sensor data reading and caching
Data preprocessing	120	57.1	Time synchronization (48ms), outlier handling (32ms), standardization (40ms)
Data fusion	20	9.5	Conflict coefficient calculation (8ms), evidence synthesis (12ms)
Early warning judgment and output	10	4.8	Trust comparison and early warning signal generation
Data transmission	60	28.6	Data transmission from edge nodes to the monitoring center
Total response time	210	100	-

In the stability analysis, the model operated continuously for 72h without failure, with a 100% trouble-free operation rate.

The performance fluctuation test results under different environmental conditions are shown in Table 6.

Table 6. Fluctuations in model performance under different environmental conditions

Environmental parameters	Test conditions	Accuracy rate (%)	False alarm rate (%)	Underreporting rate (%)	Response Time (ms)	Performance fluctuation range (%)
Ambient temperature	-10℃	95.2	3.5	1.3	205	±0.6
	25℃	95.8	3.2	1.0	200	Benchmark value
	35℃	95.5	3.3	1.2	195	±0.3
Relative humidity	30%	96.1	2.8	0.9	198	±0.3
	60%	95.8	3.2	1.0	200	Benchmark value
	90%	94.7	3.8	1.5	202	±1.1
Supply voltage	10.8V	95.6	3.4	1.1	203	±0.2
	12V	95.8	3.2	1.0	200	Benchmark value
	13.2V	95.9	3.1	0.9	197	±0.1

As can be seen from Table 6, the performance fluctuation range of the model under different environmental conditions is all ≤1.1%, demonstrating excellent stability. In a low-temperature environment of -10 ℃, the battery-powered efficiency slightly decreases, but the response time only increases by 5ms, and the accuracy rate still reaches 95.2%. Under a 90% high humidity environment, the measurement error of the pyroelectric ion sensor slightly increases. However, through the conflict correction of the fusion algorithm, the false alarm rate only rises by 0.6%, and the missed alarm rate increases by 0.5%. The core performance indicators still remain at a relatively high level.

The fusion technology proposed in this paper was compared with single pyroelectric ion monitoring, single millimeter-wave radar monitoring, and single video monitoring technologies. The results are shown in Table 7.

Table 7. Performance comparison between fusion technology and single technology solution

Technical solution	Accuracy rate (%)	False alarm rate (%)	Underreporting rate (%)	Response Time (ms)	Environmental adaptability (%)	Comprehensive performance improvement (%)
Pyroelectric ion monitoring	75.3	18.2	6.5	80	62.5	-
Millimeter radar monitoring	82.7	10.5	6.8	150	78.3	-
Video monitoring	78.5	12.3	9.2	1000	55.7	-
Fusion technology	95.8	3.2	1.0	200	91.6	32.4

As shown in Table 7, the comprehensive performance of the fusion technology in this paper has improved by 32.4% compared to the single technical solution. Among them, the accuracy rate has increased by 13.1- 20.5%, the false alarm rate has decreased by 7.3- 15.0%, the missed alarm rate has decreased by 5.5-8.2, and the environmental adaptability (accuracy in complex weather) has increased by 13.3- 35.9%. The false alarm rate of the single pyroelectric ion monitoring technology is the highest (18.2%), mainly affected by electromagnetic interference and humidity. The response time of a single video monitoring technology is the longest (1000ms), and its accuracy rate is only 55.7% in complex weather conditions. Although the single millimeter-wave radar monitoring technology has relatively good environmental adaptability, its false negative rate is relatively high (6.8%), making it difficult to identify early weak fire points. The fusion technology, through the complementarity of multi-source data, effectively compensates for the shortcomings of a single technology, significantly enhancing its overall performance.

5. Conclusions

The core innovations and research contributions of this paper are reflected in three aspects: (1) A new multi-source fusion perception paradigm for transmission line wildfire monitoring is proposed. Compared with the existing single monitoring technology and the traditional video + infrared fusion method, this study integrates the technical advantages of thermionic ionization and 77GHz millimeter-wave radar, solving the problems of lagging response and poor environmental adaptability of single technologies. The recognition accuracy in complex environments such as heavy fog and high humidity is improved by 13.3% - 35.9% compared with existing technologies; (2) The D-S evidence theory for transmission line scenarios is improved, compared with the general conflict correction method of traditional D-S, a weighted BPA correction mechanism based on the conflict coefficient $K > 0.5$ is designed, adapting to the four-level warning identification framework, and the average accuracy of the fusion algorithm is improved by 9.5% compared with traditional D-S, while maintaining a low latency of 190ms, balancing accuracy and real-time performance; (3) A quantitative four-level wildfire warning level system is established, compared with the qualitative or single-parameter warning methods in existing research, physical parameters such as ion concentration, fire point distance, and spread speed, as well as the fusion trust degree, are used as dual-dimensional judgment rules for each warning level. The F1 value of each warning level is ≥ 86.1%, achieving early identification and precise classification of wildfire hazards, providing a quantitative warning basis for transmission line wildfire prevention and control.

The core algorithms and sensing fusion paradigm of this study can provide technical references for the monitoring of other equipment in the power system and the prevention and control of forest wildfires in other fields.

In the future, targeted adaptation and optimization can be carried out based on the characteristic parameters of different fields.

Although the research has achieved certain results, there are still some shortcomings. For example, the current model does not fully consider the influence of meteorological data (such as wind speed and direction) on the spread of wildfires. In the future, a meteorological prediction model can be introduced to optimize the warning threshold, improving the forward-looking nature of the warning; secondly, the ranging accuracy of millimeter-wave radar in dense vegetation areas (vegetation coverage ≥ 80%) needs to be improved. It is possible to explore the collaborative fusion with unmanned aerial vehicle (UAV) aerial photography data to enhance the monitoring capability in complex terrains; thirdly, based on the collaborative architecture of edge computing and cloud computing, a wide-area transmission line wildfire monitoring and warning network can be constructed to achieve regional joint prevention and contr.

References

[1] Huang, H., Chen, K., Song, B., Chen, C., Li, L., & Ling, J. (2025). Susceptibility assessment of wildfire-induced transmission line tripping using a physical-Bayesian modeling approach. *Scientific Reports*. https://doi.org/10.1038/S41598-025-28345-3

[2] Chen, C., Xu, T., Cao, S., Wang, X. (2018). Study on risk assessment of trans-regional transmission lines tripping disaster induced by wildfire. *IOP Conference Series: Materials Science and Engineering*, 452(3), 1-8. https://doi.org/10.1088/1757-899X/452/3/032121

[3] Shi, S., Yao, C., Wang, S., Han, W. (2018). A Model Design for Risk Assessment of Line Tripping Caused by Wildfires. *Sensors (Basel, Switzerland)*, 18(6), 1941-1941. https://doi.org/10.3390/s18061941

[4] Li, J., Chen, J., Yu, H., Jiang, M., Lu, Z., Zhou, Y., Wang, S., & Fan, J. (2023). Wildfire monitoring technologies of transmission line corridors based on Fengyun-3E satellite imaging. *Frontiers in Energy Research*, 11, 1-12. https://doi.org/10.3389/FENRG.2023.1265516

[5] Dong, S., Ding, Y., Ma, L., He, W., & Lei, X. (2023). Design of mountain fire prevention monitoring system for transmission lines based on machine vision algorithms. *International Journal of Emerging Electric Power Systems*, 24(4), 529-539. https://doi.org/10.1515/IJEEPS-2023-0111

[6] Liang, Y., Zhou, L., Chen, J., Huang, Y., Wei, R., & Zhou, E. (2020). Monitoring and Risk Assessment of Wildfires in the Corridors of High-Voltage Transmission Lines. *IEEE Access*, 8, 170057-170069. https://doi.org/10.1109/ACCESS.2020.3023024

[7] Lu, J., Liu, Y., Zhang, G., Li, B., He, L., & Luo, J. (2018). Partition dynamic threshold monitoring technology of wildfires near overhead transmission lines by satellite. *Natural Hazards*, 94(3), 1327-1340. https://doi.org/10.1007/s11069-018-3479-5

[8] Gu, L. (2024). Railway Fire Early Warning Technology Based on Thermally Released Ions: Principle, Advantages and Application Scenario Analysis. *Information Record Materials*, 25(12), 209-211. https://doi.org/10.16009/j.cnki.cn13-1295/tq.2024.12.047

[9] Gao, G. (2024). Application and Prospect of Pyroelectric Ion Technology in Fire Early Warning of Railway Distribution Room. *Information Record Materials*, 25(12), 227-229+235. https://doi.org/10.16009/j.cnki.cn13-1295/tq.2024.12.015

[10] Soumya, A., Mohan, K. C., & Cenkeramaddi, R. L. (2023). Recent Advances in mmWave-Radar-Based Sensing, Its Applications, and Machine Learning Techniques: A Review. *Sensors*, 23(21), 8901. https://doi.org/10.3390/S23218901

[11] Mainejad, N., & Rizos, C. (2015). APPLICATION OF MULTIPLE CATEGORIES OF UNMANNED AIRCRAFT SYSTEMS (UAS) IN DIFFERENT AIRSPACES FOR BUSHFIRE MONITORING AND RESPONSE. *ISPRS - International Archives of the Photogrammetry, Remote Sensing and Spatial Information Sciences*, XL-1/W4(1), 55-60. https://doi.org/10.5194/isprsarchives-XL-1-W4-55-2015